Characterization and Gene Expression Analysis of Serum-Derived Extracellular Vesicles in Primary Aldosteronism

Characterization and gene expression analysis of serum-derived extracellular vesicles in primary aldosteronism

Jacopo Burrello, Chiara Gai, Martina Tetti, Tatiana Lopatina, Maria Chiara Deregibus, Franco Veglio, Paolo Mulatero, Giovanni Camussi, Silvia Monticone.

Division of Internal Medicine 4 and Hypertension Unit, Department of Medical Sciences, University of Turin, Turin, Italy (J.B.; M.T.; F.V.; P.M.; S.M.). Molecular Biotechnology Center, Department of Medical Sciences, University of Turin, Turin, Italy (C.G.; T.L.; M.C.D.; G.C.).

Corresponding author: Silvia Monticone, Division of Internal Medicine, Department of Medical Sciences, University of Turin Via Genova 3, 10126 Torino, Italy.

E-mail: silvia.monticone@unito.it. Phone number: +39-0116336997

Manuscript word count: 6481 including tables, references and figure captions.

Abstract word count: 249

Number of Tables: 1; Number of Figures: 5; 1 Supplemental file.

Short title: Extracellular Vesicles in Primary Aldosteronism

ABSTRACT

Patients affected by primary aldosteronism (PA) display an increased risk of cardiovascular events compared to essential hypertension (EH). Endothelial dysfunction favours initiation and progression of atherosclerosis and circulating extracellular vesicles (EVs), reflecting endothelial cell activity, could represent one of the mediators of endothelial dysfunction in these patients.

The aim of this study was to characterize circulating EVs from patients diagnosed with PA and to explore their functional significance.

Serum EVs were isolated from 12 patients with PA and 12 with EH, matched by sex, age and blood pressure, and compared with 8 NT controls. At nanoparticle tracking analysis, EVs concentration was 2.2 times higher in PA patients (P=0.033) compared with EH and a significant correlation between EV number and serum aldosterone and potassium levels was identified. Fluorescence-activated cell sorting analysis demonstrated patients with PA presented a higher absolute number of endothelial-derived EVs compared to both patients with EH and NT controls. Through EV mRNA profiling, 15 up-regulated and 4 down-regulated genes in PA patients compared to EH were identified; moreover, *EDN1* was expressed only in patients with PA. Micro-array platform was validated by qRT-PCR on 4 genes (*CASP1*, *EDN1*, *F2R*, *HMOX1*) involved in apoptosis, inflammation and endothelial dysfunction. Following unilateral adrenalectomy, EVs number and expression of *CASP1* and *EDN1* significantly decreased in PA patients ($P<0.05$). Additionally, the incubation with PA-derived EVs reduced angiogenesis and induced apoptosis in vitro. Circulating EVs might not only represent a marker of endothelial dysfunction, but also contribute themselves to vascular dysfunction in PA patients.

Keywords: extracellular vesicles, primary aldosteronism, endothelial dysfunction, endothelin-1, caspase-1.

ABBREVIATION LIST - NO, Nitric Oxide; ET-1 Endothelin-1; MR, Mineralocorticoid Receptor; PA, Primary Aldosteronism; BP, Blood Pressure; EVs, Extracellular Vesicles; EXOs, Exosomes; EH, Essential Hypertension; APA, Aldosterone Producing Adenoma; NT, Normotensive; TEM, Transmission Electron Microscopy; NTA, Nanoparticle Tracking Analysis; FACS analysis, Fluorescence-Activated Cell Sorting analysis; HMECs, Human Microvascular Endothelial Cells; GFR, Glomerular Filtration Rate; DDD, Defined Daily Dose; PRA, Plasma Renin Activity; cIMT, carotid Intima Media Thickness.

INTRODUCTION

Endothelium is the inner layer of blood vessels and plays a key role in the regulation of peripheral arterial tone and vascular homeostasis[1]. Endothelial dysfunction results from the imbalance between vasodilators, such as nitric oxide (NO), and vasoconstrictors, such as angiotensin II and endothelin-1 (ET-1)[2]. In addition to impaired vasoreactivity, endothelial failure determines a pro-inflammatory and pro-coagulatory state, favouring initiation and progression of atherosclerosis[3]; consistently, several studies demonstrated the association between endothelial dysfunction and cardiovascular events[4].

It is well known that an inappropriate aldosterone production for sodium status can induce not only arterial hypertension, but also detrimental effects on endothelium and vascular remodelling[5]. It has been reported that aldosterone treatment inhibits NO release in rat vascular smooth muscle cells[6] and that aldosterone infusion promotes, in murine models, the impairment of endothelium-dependent vasodilatation and the development of severe arterial hypertension and inflammatory response, with perivascular leukocyte infiltrate and fibrinoid necrosis of the *tunica media*[7,8]. The acute administration of aldosterone inhibits acetylcholine-induced endothelium-dependent vasodilatation in healthy volunteers[9], whereas in patients with chronic heart failure (and hence secondary hyperaldosteronism), spironolactone administration improves endothelial function by increasing NO

bioavailability[10]. Furthermore, patients with primary aldosteronism (PA) display aldosterone-related vascular inflammation and oxidative stress with endothelial dysfunction and vascular damage[11,12], which translate into increased arterial stiffness and loss of vascular reactivity[11,13]. The administration of a MR antagonist significantly improves endothelial function both in patients with PA and in control patients with resistant hypertension, independently from blood pressure (BP) decrease[11].

Extracellular vesicles (EVs) are bilayer membrane structures classified according to size and biogenesis in microvesicles and exosomes (EXOs); EXOs are the smaller and best characterized EVs, with a diameter ranging from 30 to 150 nm[14]. EVs are constitutively released by cells and they are involved in mechanisms of autocrine, paracrine and endocrine signaling through the transfer of proteins, lipids, and nucleic acids. The ability to transfer genetic information, thus influencing the behavior of target cells, makes EVs key players in inter-cellular communication[14,15]. EVs reflect the activation state of parent cell and may represent a valuable resource for the assessment of cardiovascular disease[16].

PA is a frequent cause of endocrine hypertension[17,18] and it is associated with an increased prevalence of target organ damage and cardiovascular events[19], which may at least in part depend on the endothelial dysfunction observed in these patients.

Considering serum EVs as surrogate markers of endothelial cell function, we hypothesized that they could be one of the key mediators of endothelial dysfunction and aldosterone-mediated cardiovascular injury. Therefore, the aims of the present study were: i) to characterize serum-derived EVs in patients with PA, compared to controls with essential hypertension (EH) and to normotensive (NT) healthy volunteers, ii) to analyse their mRNA cargo, and iii) to examine their potential functional effect in endothelial cell function in vitro.

METHODS

A detailed description of patient selection, EV isolation and characterization protocols and gene expression analysis is provided in the online supplement. The authors declare that all supporting data are available within the article (and its online supplementary files).

Patient Selection

Patients affected by PA, EH and NT controls were recruited at the Division of Internal Medicine and Hypertension Unit, University of Torino, Italy. Diagnosis of unilateral PA was made following the Endocrine Society guideline[17] recommendations, while diagnosis of EH was made after the exclusion of the most common forms of secondary hypertension[20]. Patients with PA were carefully matched with patients affected by EH for the main clinical parameters including age, gender and blood pressure. NT controls were healthy volunteers, without significant comorbidities. The study was approved by the local ethical committee and fully informed written consent was obtained from each patient.

EVs isolation and characterization

EVs were isolated from aliquot of serum using a charge-based precipitation method, as previously described[21]. To further purify EVs samples, we performed a second isolation step through ultracentrifugation at 100,000 g[22]. Isolated EVs were visualized by transmission electron microscopy (TEM) and then carefully characterized by Nanoparticle Tracking Analysis (NTA), Fluorescence-Activated Cell Sorting (FACS) analysis and Western Blot. FACS analysis and NTA described EVs derivation (endothelial cells, platelets or leucocytes) and the number of EVs per mL with their relative size distribution, respectively. A Western Blot on protein lysate was performed in order to confirm the presence of EVs markers on analyzed samples (CD63, TSG101 [Tumor Susceptibility Gene 101], and Flotillin-1).

Cell culture

For functional studies aimed at evaluating the effects of EVs treatment on angiogenesis and apoptosis, human microvascular endothelial cells (HMECs) were used as in vitro model and cultured as previously described[23].

Angiogenesis and apoptosis assay

In vitro formation of capillary-like structures was studied on HMECs after incubation for 24 hours with serum-derived EVs from PA patients. Apoptosis was evaluated through Annexin V assay on HMECs; cells were incubated for 24 hours with EVs from PA patients, pre-incubation with Bosentan (10 μM; Sigma) or Ac-YVAD-cmk (92.5 μM; Sigma) was used to explore the potential role of caspase-1 and endothelin on the observed functional effects.

Gene expression analysis

Gene expression analysis was performed on serum EVs (isolated from patients affected by PA before and after adrenalectomy, from patients affected by EH and from NT healthy volunteers) and on HMECs cells following EVs treatment.

RNA extraction from purified EVs and cultured HMECs cells and total RNA reverse-transcription were performed through commercially available kits (mirVana Isolation Kit, Thermo Fisher Scientific, Waltham, Massachusetts, USA; RT^2 First Strand kit, Qiagen, Hilden, Germany), according to manufacturer's instructions.

mRNA qRT-PCR array profiling was performed on serum EVs from 4 patients diagnosed with PA and 4 with EH, using a platform focused on the evaluation of 96 human genes involved in endothelial function regulation (Endothelial Cell Biology RT^2 Profiler PCR Array Format E384, *Qiagen*, Hilden, Germany). The gene expression platform was subsequently validated with qRT-PCR on serum EVs from 10 patients with PA and 10 with EH (2 patients from each group were included also in qRT-PCR array analysis) on 4 genes: *CASP1* (Caspase 1, Apoptosis-related Cysteine Peptidase), *EDN1* (Endothelin 1), *F2R* (Coagulation factor II [thrombin] receptor) and *HMOX1* (Heme Oxygenase [decycling] 1), selected on the basis of their expression profile and functional data available in

literature (see Online Supplement). qRT-PCR was performed using TaqMan gene expression assays (TermoFisher Scientific, Waltham, MA, USA) on an Applied Biosystems ABI 7500 instrument; data were analyzed through a dedicated software, with the $2^{-\Delta\Delta CT}$ relative quantification (RQ) method, using *18SrRNA* (18S ribosomal RNA) as endogenous control. A gene was considered down-regulated for FC values between 0 and 1 or up-regulated for values greater than 1.

Statistical Analysis

IBM SPSS Statistics 22 (*IBM Corp., Armonk, New York, USA*) and GraphPad PRISM 7.0a (*La Jolla, California, USA*) were used for statistical analyses. ANOVA one-way and Mann-Whitney's tests were used to compare variables with a normal or non-normal distribution, respectively. Categorical variables were compared through a chi square test (Fisher's exact test when sample size was ≤ 5). Correlations were evaluated by Pearson test (R coefficient) and regression curve analysis. *P*-values of less than 0.05 were considered significant.

RESULTS

Patient characteristics

A total of 32 subjects was included in the study: 12 patients with PA and a subtype diagnosis of APA, 12 with EH and 8 NT controls (healthy volunteers, without significant comorbidities and not taking any medication).

Patients affected by PA and patients affected by EH were carefully matched by gender, age and BP; patient characteristics and hormonal parameters are reported in Table 1. Each cohort (PA and EH) was composed of 8 males and 4 females, with a mean age of 51 ± 8 years for PA patients and 50 ± 7 for EH patients ($P = 0.809$). As expected, BP values were similar (152/94 *vs* 150/93 mmHg, respectively for patients with PA and EH; $P \geq 0.05$), patients with PA had lower potassium and PRA levels and higher aldosterone levels ($P < 0.001$ for all comparison) compared with patients with EH. Additionally, there were no significant differences between PA and EH patients also for all the other

main clinical and biochemical parameters (Table 1); none of the included patients was affected by diabetes or has experienced previous cardiovascular events (sustained arrhythmias, coronary heart disease, heart failure, or stroke) and there was no difference in cIMT, thus confirming a similar risk profile across the two cohort of patients.

EVs characterization

For each subject (NT *vs* EH *vs* PA cohort), serum-derived EVs were visualized by TEM and then systematically characterized through Western Blot for EV-markers, NTA, and FACS analysis. Representative images of isolated EVs were obtained by TEM; vesicles showed the characteristic lipid bi-layer membrane in high magnification views (Figure 1A). To confirm the presence of EVs in our samples, we performed a Western Blot analysis that demonstrated the expression of EV markers CD63, TSG101 and Flotillin-1 (Figure 1B).

At NTA, NT controls and patients with EH or PA had a similar EV-diameter (255 nm [216; 290], 231 nm [199; 264] and 241 nm [173; 259], respectively; $P = 0.315$; Figure 1C), whereas the number of EVs per mL was significantly higher both for patients with EH and PA compared to NT controls (3.6E+11 [1.7E+11; 1.7E+12] and 7.8E+11 [6.6E+11; 5.3E+12] *vs* 1.2E+11 [6.7E+10; 1.3E+11], respectively; $P = 0.001$ and $P < 0.001$) and also for patients with PA compared to EH ($P = 0.033$; Figure 1D). Diameter and vesicle size distribution were consistent with exosomes, as predominant component in all groups.

To define the origin of isolated EVs, we performed FACS analysis for three different surface markers: CD31 for endothelial cells, CD42b for platelets, and CD45 for leucocytes. In cytofluorimetric analysis, each EV passes through the flow cytometer and is detected as a distinct event; we expressed EVs concentration as the number of events detected in 60 seconds. Most EVs resulted positive for CD45 (39.8%), whereas 19.7% and 10.4% were positive for CD31 and CD42b, respectively, without significant differences in percentage distribution between the three cohorts. Patients with PA presented a higher absolute number of endothelial-derived EVs compared to both patients with EH

and NT controls (1545 [1161; 2151] *vs* 645 [508; 1174] and 913 [639; 1005] events per 60 seconds; $P = 0.005$ and $P = 0.006$, respectively). The number of leucocytes-derived EVs was higher in PA patients compared to NT controls (3091 [1970; 4531] *vs* 1397 [838; 1759] events per 60 seconds; P = 0.012), whereas we did not find differences for CD42b (649 [362; 842] *vs* 415 [313; 778] *vs* 808 [564; 979] events per 60 seconds, respectively for NT, EH and PA cohort; $P \geq 0.05$). Consistently with NTA findings, the total absolute number of events per 60 seconds was significant higher in patients with PA compared with both patients with EH and NT controls (7642 [6375; 10391] *vs* 3450 [2464; 4931] and 3960 [3304; 5066] events per 60 seconds; $P = 0.001$ and $P = 0.009$; Figure 1E).

The EV concentration was 2.2 times higher in patients with PA vs EH with both FACS analysis and NTA; furthermore, the number of EVs per mL was directly correlated with aldosterone concentration (R = 0.472; $P = 0.020$) and inversely correlated with potassium levels (R = -0.419; $P = 0.041$). Conversely, we did not find any significant correlation with PRA (R = -0.255; $P = 0.229$), systolic (R = 0.347; $P = 0.097$), or diastolic BP (R = 0.398; $P = 0.144$; Supplemental Figure S1).

After stratification for sex (Supplemental Figure S2A and Supplemental Table S1), we did not find any differences at NTA and FACS analysis, independently from the diagnosis ($P \geq 0.05$ for all comparisons).

Gene expression analysis

To investigate a potential role for EVs in aldosterone-mediated endothelial damage in patients with PA, we performed a qRT-PCR-array evaluating the expression level of a panel of 96 human genes involved in angiogenesis, vasoconstriction / vasodilatation, inflammatory response, apoptosis, cell adhesion, coagulation and platelet activation; we compared 4 patients affected by PA with 4 patients affected by EH. Considering both PA and EH cohorts, 63 genes were expressed in serum-derived EVs of at least one patient (Supplementary Table S2). Among the 19 transcripts found in EVs of at least 4 of the 8 patients included in the analysis, 4 genes were down-regulated (*CCL5* [Chemokine (C-C motif) ligand 5], *F3* [Coagulation factor III (thromboplastin)], *ITGB1* [Integrin, beta 1],

PDGFRA [PLT-derived GF receptor, alpha polypeptide]) and 15 were up-regulated (*ANGPT1* [Angiopoietin 1], *BAX* [BCL2-associated X protein], *BCL2* [B-cell CLL/lymphoma 2], *CALCA* [Calcitonin-related polypeptide alpha], *CASP1* [Caspase 1, apoptosis-related cysteine peptidase], *COL18A1* [Collagen, type XVIII, alpha 1], *ENG* [Endoglin], *F2R* [Coagulation factor II (thrombin) receptor], *HMOX1* [Heme oxygenase (decycling) 1], *IL6* [Interleukin 6], *ITGA5* [Integrin, alpha 5], *PF4* [Platelet factor 4], *PGF* [Placental growth factor], *PTGIS* [Prostaglandin I2 synthase], *VEGFA* [Vascular endothelial growth factor A]); noteworthy, *EDN1* [Endothelin 1] was expressed in only 3 patients with a diagnosis of PA. The hierarchical clustering analysis is reported in Figure 2. After an initial unbiased transcriptional screening, we validated our results through a target gene approach; we performed qRT-PCR on 4 selected genes (*CASP1, EDN1, F2R, HMOX1*) in 10 patients with diagnosis of unilateral PA, 10 with EH and 8 NT healthy controls. We selected the above-mentioned genes considering the expression profile in EVs and current available knowledge on their functional role (see Online Supplement).

After normalization for *18SrRNA* expression and correction for the number of EVs per mL, we calculated the fold-change (FC) as the ratio between the RQ (Relative quantification coefficient) of PA or EH patients compared to NT controls (Figure 3). *CASP1* and *EDN1* were up-regulated in patients with PA compared with either EH or NT controls (FC = 12.0 and FC = 33.9, $P = 0.023$ and $P = 0.006$; FC = 18.3 and FC = 19.2, $P = 0.035$ and $P = 0.043$, respectively), *HMOX1* was up-regulated in patients with PA compared to NT controls (FC = 9.1, $P = 0.016$) and in EH compared to NT (FC = 3.8, $P = 0.043$), whereas we did not find significant differences for *F2R* ($P \geq 0.05$ for all comparisons). To exclude a potential confounding effect due to sex, we stratified qRT-PCR results, and we did not find any difference between males and females in the expression of *CASP1*, *EDN1*, *F2R* and *HMOX1* (Supplemental Figure S2 B-E and Supplemental Table S1).

Evaluation of patients affected by PA at follow-up

The choice of including only patients with an unequivocal diagnosis of unilateral PA allowed us to perform a direct comparison of the same patients before and after curative surgery, in order to identify potential aldosterone-induced modifications in EVs profiling and to avoid potential overlapping between patients with mild bilateral forms of PA and low-renin essential hypertension. Of the 12 patients with APA, 9 underwent unilateral adrenalectomy and 4 were re-evaluated 1 year after surgery. Biochemical cure of PA was achieved in all 4 patients (resulting in normalization of aldosterone/renin ratio and potassium levels[24]), and BP decreased to normal values (even if in presence of antihypertensive therapy in 2 of the 4 patients).

Interestingly, following adrenalectomy, the total number of EVs per mL was significantly reduced (5.8E+11 [5.7E+11; 6.7E+11] *vs* 2.7E+11 [1.3E+11; 3.2E+11]; $P = 0.029$; Figure 4A), without significant differences of EVs diameter at NTA (264 nm [189; 276] *vs* 198 nm [188; 225], $P = 0.343$; Figure 4B) and EVs origin at FACS analysis (1647 [772; 2277] *vs* 3263 [1947; 4886] CD31+ events per 60 seconds, $P = 0.114$; 776 [594; 1413] *vs* 1723 [1056; 1916] CD42b+ events per 60 seconds, $P = 0.115$; 4031 [1521; 4423] *vs* 3364 [1377; 4797] CD45+ events per 60 seconds, $P = 0.686$).

Similarly, qRT-PCR analysis revealed that the expression of *CASP1* and *EDN1* was significantly reduced (FC = 0.06 – $P = 0.027$ and FC = 0.04 – $P = 0.029$, respectively; Figure 4C) after surgery.

Gene expression studies, angiogenesis and apoptosis assays on HMECs

To evaluate the biological significance of our findings we investigate the functional role of PA patient serum-derived EVs *in vitro*. Human microvascular endothelial cells (HMECs) were incubated for 24 hours with EVs, then qRT-PCR, angiogenic assay, and apoptosis assays were performed. Selective caspase-1 inhibitor (Ac-YVAD-cmk) and endothelin receptor type A and B non-selective inhibitor (bosentan) were used to evaluate the potential involvement of caspase-1 and endothelin as bioactive effectors of endothelial damage in our in vitro model.

After the incubation with EVs, we observed a non-significant increase of the expression of *CASP1* (FC = 1.2), *EDN1* (FC = 2.9), *F2R* (FC = 3.8), and *HMOX1* (FC = 2.9) in HMECs compared to non-

treated cells. In vitro formation of capillary-like structures was studied on the same model and expressed as arbitrary unit (a.u.); the angiogenic assay demonstrated a significant reduction of tube length after treatment with EVs *vs* non-treated cells (11,187 a.u. [10,385; 11,955] *vs* 12,238 a.u. [11,975; 12,904]; $P = 0.019$; Figure 5A); cells treated with bosentan did not display significant differences with controls and EV-treated cells (11,541 a.u. [10,796; 13,587]).

Finally, apoptosis was evaluated through Annexin V assay; the percentage of live cells decreased following the incubation with EVs (82.9 [81.1-83.0] *vs* 76.3 [71.1-79.3], respectively for non-treated cells and PA-derived EVs treated cells; $P = 0.029$; Figure 5B); the observed effect was not reverted by pre-treatment with the selective caspase-1 inhibitor, Ac-YVAD-cmk (74.9 [70.3; 78.4]).

DISCUSSION

This study shows, for the first time, that serum EVs profiling differs significantly between patients affected by unilateral PA and carefully matched patients affected by EH and that PA-derived EVs can influence endothelial cell function, promoting apoptosis and inhibiting angiogenesis in vitro.

In our cohort, the total number of EVs mainly derived from leucocytes and endothelial cells, is significantly higher in patients with PA compared to both EH and NT controls, directly correlates with aldosterone and inversely with potassium levels.

In peripheral blood of healthy subjects, EVs mainly derive from platelets[25], while the percentage of endothelial and leucocyte-derived EVs raises in pathological conditions such as atherosclerosis[26]. An increased number of circulating EVs has been reported in patients with acute coronary syndrome[27], chronic renal failure[28], diabetes[29], and pre-eclampsia[30]. The concentration of endothelial- and platelet-derived EVs has been observed to be higher also in hypertensive patients compared to normotensive controls and the number of EVs per mL was proportional to systolic and diastolic BP[31].

In the present study patients with PA displayed a higher serum-derived EVs number compared with blood pressure-matched patients affected by EH, which could be due to a direct effect of aldosterone

on EVs number, or alternatively, it could be the consequence of a more severe PA-associated endothelial damage.

To further investigate the potential role of EVs in aldosterone-mediated endothelial damage, we performed a targeted mRNA profiling analysis on genes involved in the regulation of endothelial function. Among genes differentially expressed in PA compared to EH patients, we focused on *CASP1* and *EDN1*, whose up-regulation was confirmed by qRT-PCR not only in EVs from patients with PA compared with patients affected by EH, but also compared with a cohort of NT controls.

Unilateral adrenalectomy is the treatment of choice for patients who display lateralized aldosterone overproduction, allowing to achieve biochemical cure of the disease in the vast majority of cases[24]. In order to further demonstrate a direct and independent effect of aldosterone on EVs profiling, 4 out of the 12 included patients affected by PA were re-evaluated after surgery. Following unilateral adrenalectomy, which resulted in the biochemical cure of PA, the number of EVs per mL and the expression of *CASP1* and *EDN1* significantly decreased compared to the pre-operative status indicating that these findings were mediated by the condition of aldosterone excess.

CASP1 encodes for caspase-1, a cysteine-aspartic acid protease, which plays a central role in the execution-phase of apoptosis. Recently, the involvement of caspase-1 in aldosterone-induced vascular endothelial damage[32] and renal tubulointerstitial fibrosis[33,34], through *in vitro* and *in vivo* studies, has been reported. In mice, aldosterone infusion increased the expression of caspase-1 and two inflammasome components, ASC (Apoptosis-associated Speck-like protein Caspase-recruitment domain) and NLRP-3 (Nucleotide-binding domain, Leucine-Rich-containing family, Pyrin domain-containing-3), effects that were specifically abolished by the mineralocorticoid receptor antagonist eplerenone[33]. The inflammasome complex activates caspase-1, which converts the precursors of IL-1β and IL-18 to their active forms, inducing an inflammatory response[35]. Confirming these results, leukocytes from a healthy volunteer treated in vitro with aldosterone displayed an increased expression of *NLRP-3* and the activation of caspase-1 with increased levels of IL-1β in the

supernatant[32]. It has been suggested that endothelial apoptosis might play a role in the early phase of atherosclerosis[36], therefore PA-derived EVs, carrying mRNA encoding for caspase-1, could contribute to the enhanced endothelial dysfunction and hence the increased cardiovascular risk observed in these patients[19].

EDN1 encodes a pre-pro-protein, which is processed through proteolysis in endothelial cells to the potent vasoconstrictor ET-1. ET-1 stimulates aldosterone production *in vitro* by primary culture of aldosterone-producing adenoma cells through binding to its receptors, ET-A and ET-B (Endothelin receptors Type A and B)[37]. Indeed, ET-1 was reported to be able to enhance angiotensin-II and ACTH-dependent up-regulation of *CYP11B2*, stimulating the synthesis of aldosterone[38]. On the other hand, aldosterone induces the release of ET-1 from murine renal collecting duct cells through the epigenetic modification of chromatin structure around regulatory elements of *EDN1*, by MR activation[39]. In addition, murine models infused with aldosterone develop functional and structural vascular remodeling with increased levels of ET-1, systemic oxidative stress, *tunica intima* thickening, and deposition of collagen and fibronectin in the extra-cellular matrix[8]; spironolactone and an ET-A blocker prevented all these effects, suggesting that the detrimental action of aldosterone at vascular level is mediated not only by the mineralocorticoid receptor activation but also by ET-1 and its receptors[8]. Nevertheless, the role of ET-1 in PA patients remains unclear; while some authors reported an increased production of aldosterone in subjects undergoing co-infusion of ACTH and ET-1[40], others did not find any difference in circulating levels of ET-1 in patients with PA compared to controls with EH[41].

We also evaluated in an *in vitro* model the potential biological significance of our findings through apoptosis and angiogenetic assays. Impairment of angiogenesis is one of the key players involved in the development of endothelial dysfunction in ageing vasculature, through different mechanisms which include reduced nitric oxide bioavailability and apoptosis[42].

The incubation of endothelial cells with EVs derived from PA patients resulted in a significant reduction in live cells percentage (pro-apoptotic effect) and capillary formation (anti-angiogenic effect), while the expression of *CASP1*, *EDN1*, *F2R* and *HMOX1* was not significantly affected. Pre-incubation with caspase-1 and endothelin inhibitor bosentan failed to revert the effects of EVs on angiogenesis and apoptosis, which are likely to result from multiple signaling processes including the delivery of other mRNA species, miRNA, cytokines, rather than from a single mediator.

The main limitation of our study is that we were not able to show a direct effect of the increased levels of caspase-1 and endothelin-1 on endothelial function in vitro; however, it should be noted that the complex pathophysiological conditions of patients with PA, where endothelium is long-term exposed to increased aldosterone levels in a context of inappropriate sodium and increased blood pressure, cannot be reproduced *in vitro*. Moreover, we enrolled a relatively low number of patients and our findings should be confirmed on a larger cohort.

In conclusion, our data suggest that in patients affected by PA, aldosterone excess can influence the number and the gene expression profiling of serum EVs, which reflect the enhanced endothelial damage observed in these patients. Additionally, it is possible to speculate that also in patients affected by PA, circulating EVs might be part of a feedforward system[43], where aldosterone promotes endothelial damage and EVs release, which in turn contribute themselves to vascular dysfunction by inducing apoptosis and inhibiting angiogenesis through a multifaceted mechanism.

PERSPECTIVES

Although a great deal of work remains to translate *in vitro* findings to the clinical practice, accumulating evidence suggest that EVs may be more than just biomarkers, but bioactive effectors of vascular damage. Preliminary findings from our study indicate that patients affected by PA display a unique and distinct EVs profiling, and that PA-derived EVs can influence endothelial cell function *in vitro*, thereby potentially contributing to the cardiovascular risk in these patients. Further research

efforts should be devoted to fully elucidate the role and importance of serum EVs on endothelial dysfunction and their interaction with other risk factors in patients affected by PA.

ACKNOWLEDGMENTS - All the authors contributed extensively to the work presented in this manuscript. J.B., S.M. and P.M. conceived the study. J.B. and M.T. selected the patients and collected clinical information and samples. J.B., C.G., M.T., and T.L. performed EVs characterization and gene expression analysis. J.B. performed statistical analysis. J.B. and S.M. wrote the manuscript with input from all authors. C.G., T.L., M.C.D., F.V., P.M. and G.C. critically revised the manuscript.

Source(s) of Funding. This work was supported by a grant from Ministero dell'Istruzione dell'Università e della Ricerca (MIUR; ex-60% 2018 to S. M.)

Conflict(s) of Interest/Disclosure(s): M.C.D. and G.C. are named as inventors in patents related to extracellular vesicles.

REFERENCES

1. Hadi HA, Carr CS, Al Suwaidi J. Endothelial dysfunction: cardiovascular risk factors, therapy, and outcome. *Vasc Health Risk Manag.* 2005;1:183-198.
2. Lerman A, Burnett JC Jr. Intact and altered endothelium in regulation of vasomotion. *Circulation*. 1992;86:12-19.
3. Davignon J, Ganz P. Role of endothelial dysfunction in atherosclerosis. *Circulation.* 2004;109:27-32.
4. Lerman A, Zeiher AM. Endothelial function: cardiac events. *Circulation.* 2005;111:363-368.
5. Endemann DH, Touyz RM, Iglarz M, Savoia C, Schiffrin EL. Eplerenone prevents salt-induced vascular remodeling and cardiac fibrosis in stroke-prone spontaneously hypertensive rats. *Hypertension*. 2004;43:1252-1257.
6. Ikeda U, Kanbe T, Nakayama I, Kawahara Y, Yokoyama M, Shimada K. Aldosterone inhibits nitric oxide synthesis in rat vascular smooth muscle cells induced by interleukin-1 beta. *Eur J Pharmacol.* 1995;290:69-73.
7. Rocha R, Rudolph AE, Frierdich GE, Nachowiak DA, Kekec BK, Blomme EA, McMahon EG, Delyani JA. Aldosterone induces a vascular inflammatory phenotype in the rat heart. *Am J Physiol Heart Circ Physiol.* 2002;283:1802-1810.
8. Pu Q, Neves MF, Virdis A, Touyz RM, Schiffrin EL. Endothelin antagonism on aldosterone-induced oxidative stress and vascular remodeling. *Hypertension*. 2003;42:49-55.
9. Farquharson CA, Struthers AD. Aldosterone induces acute endothelial dysfunction in vivo in humans: evidence for an aldosterone-induced vasculopathy. *Clin Sci (Lond).* 2002;103:425-431.
10. Farquharson CA, Struthers AD. Spironolactone increases nitric oxide bioactivity, improves endothelial vasodilator dysfunction, and suppresses vascular angiotensin I/angiotensin II conversion in patients with chronic heart failure. *Circulation.* 2000;101:594-597.

11. Nishizaka MK, Zaman MA, Green SA, Renfroe KY, Calhoun DA. Impaired endothelium-dependent flow-mediated vasodilation in hypertensive subjects with hyperaldosteronism. *Circulation*. 2004;109:2857-2861.
12. Matsumoto T, Oki K, Kajikawa M, et al. Effect of aldosterone-producing adenoma on endothelial function and Rho-associated kinase activity in patients with primary aldosteronism. *Hypertension*. 2015;65:841-848.
13. Bernini G, Galetta F, Franzoni F, Bardini M, Taurino C, Bernardini M, Ghiadoni L, Bernini M, Santoro G, Salvetti A. Arterial stiffness, intima-media thickness and carotid artery fibrosis in patients with primary aldosteronism. *J Hypertens*. 2008;26:2399-2405.
14. Yáñez-Mó M, Siljander PR, Andreu Z, et al. Biological properties of extracellular vesicles and their physiological functions. *J Extracell Vesicles*. 2015;4:27066.
15. Ratajczak J, Miekus K, Kucia M, Zhang J, Reca R, Dvorak P, Ratajczak MZ. Embryonic stem cell-derived microvesicles reprogram hematopoietic progenitors: evidence for horizontal transfer of mRNA and protein delivery. *Leukemia*. 2006;20:847-856.
16. Helbing T, Olivier C, Bode C, Moser M, Diehl P. Role of microparticles in endothelial dysfunction and arterial hypertension. *World J Cardiol*. 2014;6:1135-1139.
17. Funder JW, Carey RM, Mantero F, Murad MH, Reincke M, Shibata H, Stowasser M, Young WF Jr. The Management of Primary Aldosteronism: Case Detection, Diagnosis, and Treatment: An Endocrine Society Clinical Practice Guideline. *J Clin Endocrinol Metab*. 2016;101:1889-1916.
18. Monticone S, Burrello J, Tizzani D, Bertello C, Viola A, Buffolo F, Gabetti L, Mengozzi G, Williams TA, Rabbia F, Veglio F, Mulatero P. Prevalence and Clinical Manifestations of Primary Aldosteronism Encountered in Primary Care Practice. *J Am Coll Cardiol*. 2017;69:1811-1820.
19. Monticone S, D'Ascenzo F, Moretti C, Williams TA, Veglio F, Gaita F, Mulatero P. Cardiovascular events and target organ damage in primary aldosteronism compared with

essential hypertension: a systematic review and meta-analysis. *Lancet Diabetes Endocrinol.* 2018;6:41-50.

20. Williams B, Mancia G, Spiering W, et al., ESC Scientific Document Group. 2018 ESC/ESH Guidelines for the management of arterial hypertension. Eur Heart J. 2018;39:3021 – 3104.
21. Deregibus MC, Figliolini F, D'Antico S, Manzini PM, Pasquino C, De Lena M, Tetta C, Brizzi MF, Camussi G. Charge-based precipitation of extracellular vesicles. *Int J Mol Med.* 2016;38:1359-1366.
22. Witwer KW, Buzás EI, Bemis LT, Bora A, Lässer C, Lötvall J, Nolte-'t Hoen EN, Piper MG, Sivaraman S, Skog J, Théry C, Wauben MH, Hochberg F. Standardization of sample collection, isolation and analysis methods in extracellular vesicle research. *J Extracell Vesicles*. 2013;2.
23. Zanone MM, Favaro E, Conaldi PG, Greening J, Bottelli A, Perin PC, Klein NJ, Peakman M, Camussi G. Persistent infection of human microvascular endothelial cells by coxsackie B viruses induces increased expression of adhesion molecules. J Immunol. 2003;171:438-446.
24. Williams TA, Lenders JWM, Mulatero P, et al., Primary Aldosteronism Surgery Outcome (PASO) investigators. Outcomes after adrenalectomy for unilateral primary aldosteronism: an international consensus on outcome measures and analysis of remission rates in an international cohort. Lancet Diabetes Endocrinol. 2017;5:689-699.
25. Müller G. Microvesicles/exosomes as potential novel biomarkers of metabolic diseases. *Diabetes Metab Syndr Obes*. 2012;5:247-282.
26. Leroyer AS, Isobe H, Lesèche G, Castier Y, Wassef M, Mallat Z, Binder BR, Tedgui A, Boulanger CM. Cellular origins and thrombogenic activity of microparticles isolated from human atherosclerotic plaques. *J Am Coll Cardiol*. 2007;49:772-777.
27. Bernal-Mizrachi L, Jy W, Jimenez JJ, Pastor J, Mauro LM, Horstman LL, de Marchena E, Ahn YS. High levels of circulating endothelial microparticles in patients with acute coronary syndromes. *Am Heart J*. 2003;145:962-970.

28. Amabile N, Guérin AP, Leroyer A, Mallat Z, Nguyen C, Boddaert J, London GM, Tedgui A, Boulanger CM. Circulating endothelial microparticles are associated with vascular dysfunction in patients with end-stage renal failure. *J Am Soc Nephrol.* 2005;16:3381-3381.
29. Sabatier F, Darmon P, Hugel B, Combes V, Sanmarco M, Velut JG, Arnoux D, Charpiot P, Freyssinet JM, Oliver C, Sampol J, Dignat-George F. Type 1 and type 2 diabetic patients display different patterns of cellular microparticles. *Diabetes*. 2002;51:2840-2845.
30. González-Quintero VH, Jiménez JJ, Jy W, Mauro LM, Hortman L, O'Sullivan MJ, Ahn Y. Elevated plasma endothelial microparticles in preeclampsia. *Am J Obstet Gynecol.* 2003;189:589-593.
31. Preston RA, Jy W, Jimenez JJ, Mauro LM, Horstman LL, Valle M, Aime G, Ahn YS. Effects of severe hypertension on endothelial and platelet microparticles. *Hypertension*. 2003;41:211-217.
32. Bruder-Nascimento T, Ferreira NS, Zanotto CZ, et al. NLRP3 Inflammasome Mediates Aldosterone-Induced Vascular Damage. *Circulation.* 2016;134:1866-1880.
33. Kadoya H, Satoh M, Sasaki T, Taniguchi S, Takahashi M, Kashihara N. Excess aldosterone is a critical danger signal for inflammasome activation in the development of renal fibrosis in mice. *FASEB J*. 2015;29:3899-3910.
34. Ding W, Guo H, Xu C, Wang B, Zhang M, Ding F. Mitochondrial reactive oxygen species-mediated NLRP3 inflammasome activation contributes to aldosterone-induced renal tubular cells injury. *Oncotarget*. 2016;7:17479-17491.
35. Martinon F, Burns K, Tschopp J. The inflammasome: a molecular platform triggering activation of inflammatory caspases and processing of proIL-beta. *Mol Cell.* 2002;10:417-426.
36. Haunstetter A, Izumo S. Apoptosis: basic mechanisms and implications for cardiovascular disease Circ Res, 1998;82:1111-1129.
37. Rossi GP, Andreis PG, Neri G, Tortorella C, Pelizzo MR, Sacchetto A, Nussdorfer GG. Endothelin-1 stimulates aldosterone synthesis in Conn's adenomas via both A and B receptors

coupled with the protein kinase C- and cyclooxygenase-dependent signaling pathways. *J Investig Med*. 2000;48:343-350.

38. Rosolowsky LJ, Campbell WB. Endothelin enhances adrenocorticotropin-stimulated aldosterone release from cultured bovine adrenal cells. *Endocrinology*. 1990;126:1860-1866.
39. Welch AK, Jeanette Lynch I, Gumz ML, Cain BD, Wingo CS. Aldosterone alters the chromatin structure of the murine endothelin-1 gene. *Life Sci*. 2016;159:121-126.
40. Vierhapper H, Nowotny P, Waldhäusl W. Effect of endothelin-1 in man: impact on basal and adrenocorticotropin-stimulated concentrations of aldosterone. *J Clin Endocrinol Metab*. 1995;80:948-951.
41. Veglio F, Melchio R, Rabbia F, Chiandussi L. Plasma immunoreactive endothelin-1 in primary hyperaldosteronism. *Am J Hypertens*. 1994;7:559-561.
42. Ungvari Z, Tarantini S, Kiss T, Wren JD, Giles CB, Griffin CT, Murfee WL, Pacher P, Csiszar A. Endothelial dysfunction and angiogenesis impairment in the ageing vasculature. Nat Rev Cardiol. 2018;15:555-565.
43. Burger D, Montezano AC, Nishigaki N, He Y, Carter A, Touyz RM. Endothelial microparticle formation by angiotensin II is mediated via Ang II receptor type I/NADPH oxidase/ Rho kinase pathways targeted to lipid rafts. Arterioscler Thromb Vasc Biol. 201;31:1898-1907.

NOVELTY AND SIGNIFICANCE

What is New?

This is the first study which characterizes serum-derived EVs from patients with PA in comparison with EVs from patients with EH (matched by age, gender and BP values) and NT healthy volunteers and provides evidence of a functional effect of PA-derived EVs on endothelial cells *in vitro*.

What is Relevant?

Our results demonstrate that patients with PA have a higher number of circulating EVs, mainly derived from leucocytes and endothelial cells. PA-derived EVs are enriched in *CASP1* and *EDN1* transcripts, suggesting their involvement in the development of endothelial dysfunction displayed by these patients. The expression of *CASP1* and *EDN1* was significantly reduced after unilateral adrenalectomy and endothelial cells displayed increased apoptosis and reduced angiogenesis after incubation with EVs.

Summary

PA affects 5-10% of hypertensive patients and is associated with an increased prevalence of cardiovascular events; endothelial dysfunction is considered a pre-clinical marker of aldosterone-mediated cardiovascular disease. Reflecting endothelial cells functional state, EVs could represent a marker of aldosterone-associated accelerated target organ damage.

Figures and Figure legends

Figure 1 *– Serum-derived extracellular vesicles (EVs) characterization*

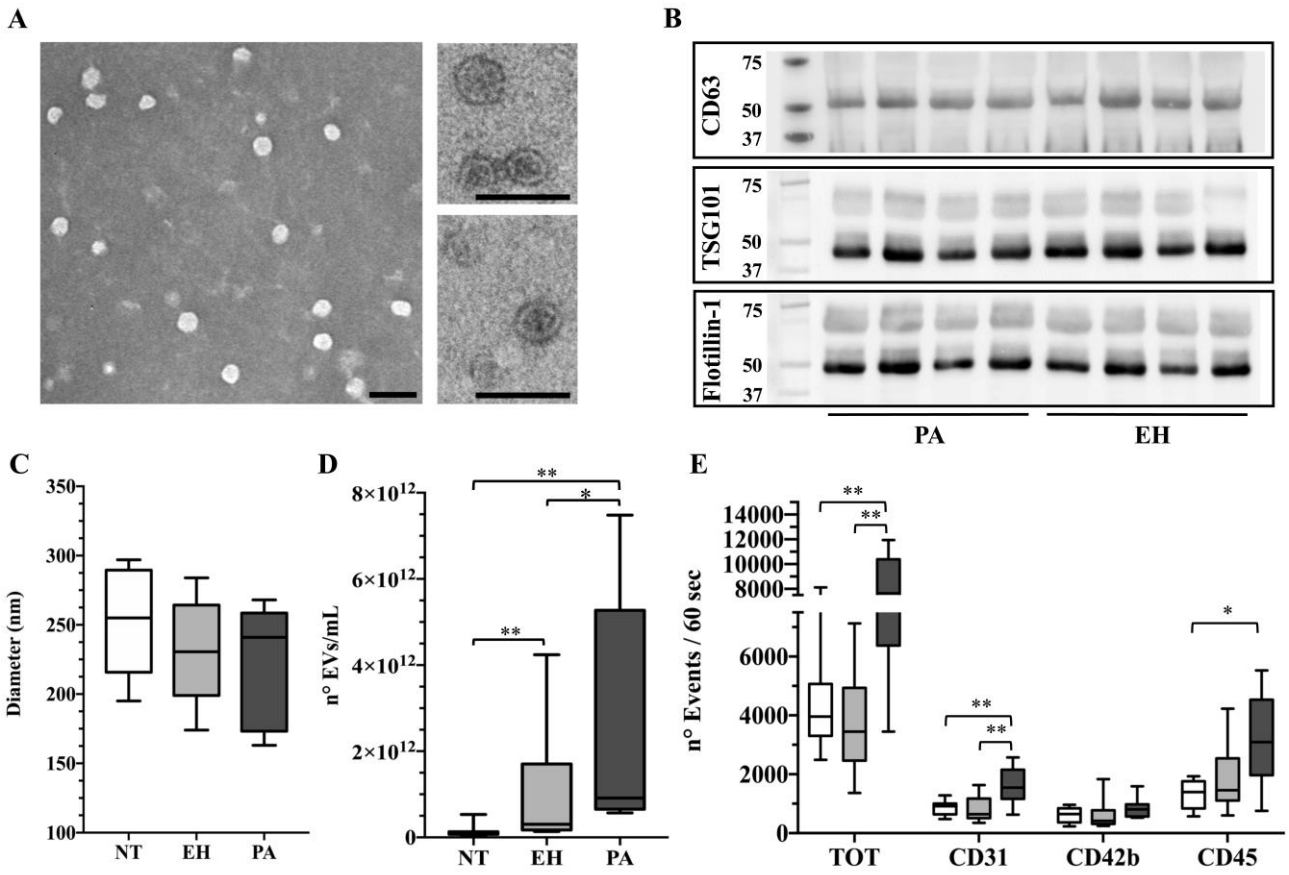

Legend to Figure 1 – Characterization of serum-derived EVs from patients with a diagnosis of PA (Primary Aldosteronism; dark grey boxes; n = 12), or EH (Essential Hypertension; light grey boxes; n = 12), compared to normotensive (NT) healthy controls (white boxes; n = 8). (A) Transmission electron microscopy: representative images of EVs purified from serum by charge-based precipitation. Right panel magnification x100k, left panels magnification x160k; bars: 100 nm; (B) Western Blot Analysis of CD63 (35-55 kDa), TSG101 (45 kDa) and Flotillin-1 (45 kDa); representative blots are shown for 4 patients with PA and 4 with EH. (C) Diameter of EVs in nm at NTA (Nanoparticle Tracking Analysis); (D) Quantification of EVs (n° EVs per mL) at NTA; (E) FACS analysis for CD31, CD42b and CD45; the box plot represents the number of events in 60

seconds. In panels C, D and E, the horizontal line indicates the median and box and bars represent the 25^{th} to 75^{th} and the 5^{th} to 95^{th} percentiles, respectively; * $P < 0.05$; ** $P < 0.01$.

Figure 2 *– mRNA qRT-PCR-array profiling*

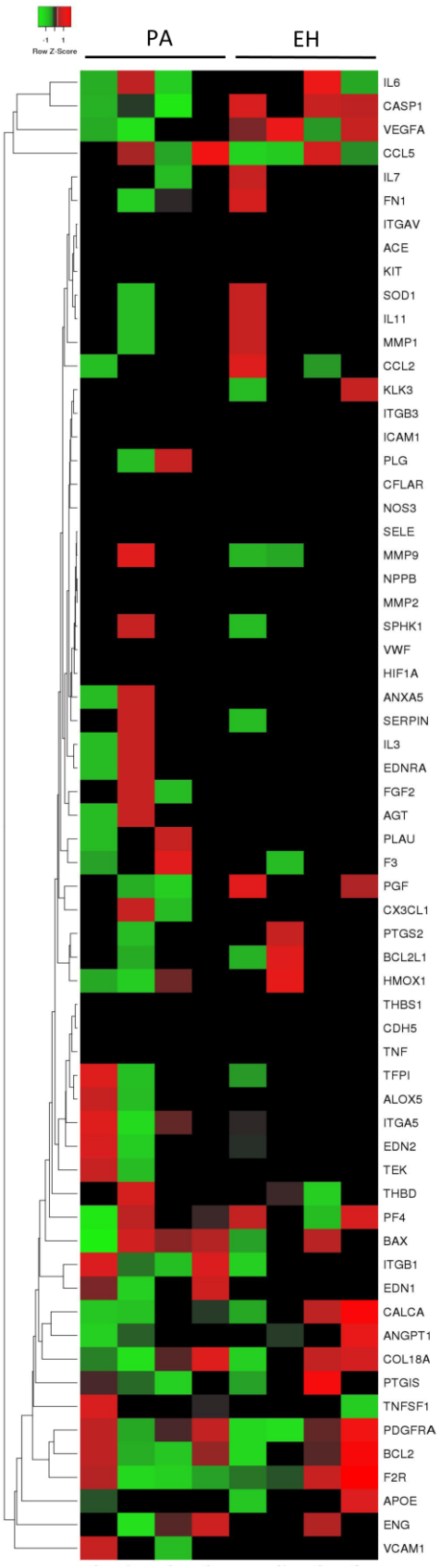

Legend to Figure 2 – Heat map showing hierarchical cluster analysis of 63 genes expressed in serum-derived EVs from patients with diagnosis of PA (Primary Aldosteronism) compared to patients with

EH (Essential Hypertension). Up-regulated transcripts are reported in green and down-regulated transcripts in red, with darker shades for intermediate values. In black are represented not expressed genes. Patients are represented on columns (4 patients with PA on the left and 4 patients with EH on the right), whereas genes are represented on lines and labeled on the right. The log color scale is shown on the top.

Figure 3 – *qRT-PCR*

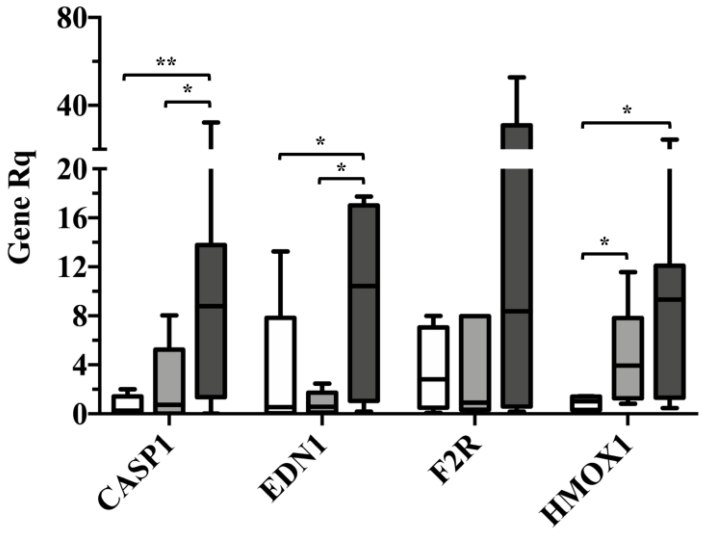

Legend to Figure 3 – Validation of gene expression profile by real-time PCR. TaqMan gene expression assays were used in qRT-PCR, performed in triplicate, to determine fold changes (FC) of expression levels in PA (Primary Aldosteronism; dark grey boxes; n = 10) patients compared to EH (Essential Hypertension; light grey boxes; n = 10) and to normotensive (NT) healthy controls (n = 8). *CASP1*, *EDN1*, *F2R* and *HMOX1* levels were evaluated using *18SrRNA* as endogenous reference gene. RQ (Relative Quantification) are corrected for the n° of EVs/mL for each sample. The horizontal line indicates the median and box and bars represent the 25th to 75th and the 5th to 95th percentiles, respectively; * $P < 0.05$; ** $P < 0.01$.

Figure 4 *– Evaluation PA patients following unilateral adrenalectomy*

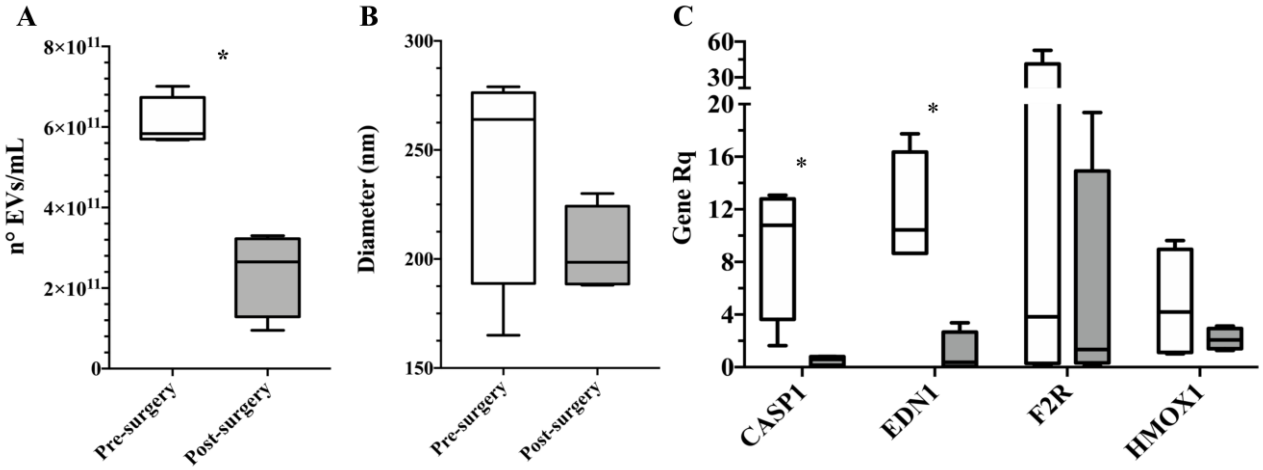

Legend to Figure 4 – Characterization of serum-derived EVs from patients with PA before (pre-surgery; white boxes) and after (post-surgery; grey boxes) unilateral adrenalectomy (n = 4). (A) Quantification of EVs (n° EVs per mL) at NTA; (B) Diameter of EVs in nm at NTA (Nanoparticle Tracking Analysis); (C) Gene expression profile by real-time PCR before and after unilateral adrenalectomy; *CASP1*, *EDN1*, *F2R* and *HMOX1* levels were evaluated using *18SrRNA* as endogenous reference gene. RQ (Relative Quantification) are corrected for the n° of EVs/mL for each sample. The horizontal line indicates the median and box and bars represent the 25th to 75th and the 5th to 95th percentiles, respectively; * $P < 0.05$.

Figure 5 *– Functional effects of PA and EH patient-derived EVs*

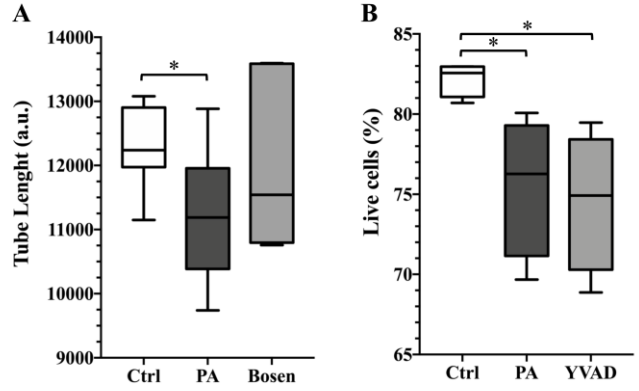

Legend to Figure 5 – Serum-derived EVs treatment effects on human microvascular endothelial cells (HMECs). HMECs were incubated with EVs derived from PA (dark grey boxes) at the dose of 1.1×10^5 EVs/cell; non-treated cells were used as negative control (white boxes), whereas bosentan or Ac-YVAD-cmk were tested to block the potential effects of *EDN1* and *CASP1* carried by EVs, respectively in the angiogenesis and in the apoptosis assays (light grey boxes). (A) In vitro angiogenic assay on growth factor-reduced Matrigel; length of capillary-like structures (expressed as a.u., arbitrary unit) after 24 hours; Bosen = bosentan (B) Annexin V apoptosis assay; percentage of live cells after 24 hours; YVAD = Ac-YVAD-cmk. The horizontal line indicates the median and box and bars represent the 25^{th} to 75^{th} and the 5^{th} to 95^{th} percentiles, respectively; * $P < 0.05$. Represented values are median and interquartile range of 3 independent experiments.

Table 1 *– Patients characteristics*

Variable	**PA** (n = 12)	**EH** (n = 12)	***P*-value**
Sex (M/F) (n; %)	8/4 (66.7/33.3)	8/4 (66.7/33.3)	1.000
Age (years)	51 ± 8.0	50 ± 7.0	0.809
Duration of HTN (years)	3.0 [1.0-15.0]	3.5 [1.0-8.0]	0.799
DDD (Defined Daily Dose)	2.0 [2.0-3.8]	2.5 [0.1-3.4]	0.590
Weight (Kg)	87 ± 18.4	81 ± 12.2	0.356
BMI (Kg/sqm)	27.1 ± 4.5	26.8 ± 2.6	0.800
Systolic BP (mmHg)	152 ± 13.2	150 ± 10.9	0.529
Diastolic BP (mmHg)	94 ± 7.4	93 ± 6.9	0.700
Potassium (mEq/L)	3.6 ± 0.4	4.3 ± 0.3	< 0.001
Aldosterone (ng/dL)	28.3 [23.5 - 42.9]	9.4 [6.0 - 14.8]	< 0.001
PRA (ng/mL/h)	0.3 [0.1 - 0.6]	1.3 [0.8 - 3.8]	< 0.001
Creatinine (mg/dL)	0.9 ± 0.14	0.9 ± 0.16	0.590
GFR (mL/min)	118 ± 28.2	107 ± 18.0	0.267
Glycemia (mg/dL)	91 ± 10.1	90 ± 10.5	0.695
Total Cholesterol (mg/dL)	183 ± 24.9	186 ± 17.6	0.743
Triglycerides (mg/dL)	108 ± 49.6	112 ± 36.4	0.802
HDL (mg/dL)	47 ± 7.9	48 ± 12.4	0.816
Carotid IMT (mm)	0.8 [0.7-1.0]	0.8 [0.7-0.9]	0.447
Smoking Status (Yes)	3 (25.0)	4 (33.3)	0.653
ASA theraphy (Yes)	1 (8.3)	1 (8.3)	1.000
Diabetes (Yes)	0 (0.0)	0 (0.0)	1.000
Metabolic Syndrome (Yes)	2 (16.7)	2 (16.7)	1.000
Cardiovascular Events (Yes)	0 (0.0)	0 (0.0)	1.000

Legend to Table 1 – Clinical and biochemical characteristics of patients affected by PA (Primary Aldosteronism) or EH (Essential Hypertension). M/F (Male/Female), HTN (Hypertension), DDD (Defined Daily Dose), BP (Blood Pressure), PRA (Plasma Renin Activity), GFR (Glomerular Filtration Rate), cIMT (carotid intima media), ASA (Acetyl-Salicylic Acid). *P*-values of less than 0.05 were considered significant.

Online-only Supplement

Characterization and gene expression analysis of serum-derived extracellular vesicles in primary aldosteronism

Jacopo Burrello, Chiara Gai, Martina Tetti, Tatiana Lopatina, Maria Chiara Deregibus, Franco Veglio, Paolo Mulatero, Giovanni Camussi, Silvia Monticone.

Division of Internal Medicine, Department of Medical Sciences, University of Turin, Turin, Italy (J.B.; M.T.; F.V.; P.M.; S.M.). Department of Medical Sciences, Molecular Biotechnology Center, University of Turin, Turin, Italy (C.G.; T.L.; M.C.D.; G.C.).

Index

EXTENDED METHODS

Patient Selection

The 24 patients included in our analysis (12 with diagnosis of primary aldosteronism, PA, and 12 with essential hypertension, EH) were referred to the Division of Internal Medicine and Hypertension Unit, University of Torino.

Diagnosis of PA was made according to the Endocrine Society (ES) guideline[1]. The cut-offs used for the screening test were an aldosterone-to-renin ratio (ARR) greater than 30 ng/dL/pg*mL^{-1}*h^{-1}, together with and aldosterone concentration > 10 ng/dL. Patients with a positive screening test underwent intravenous saline loading test (using a post-test aldosterone concentration greater than 5 ng/dL, as cut-off) or captopril challenge test when acute plasma volume expansion was contraindicated (using a post-test ARR greater than 30 ng/dL/pg*mL^{-1}*h^{-1}, as cut-off). Patients with a confirmed diagnosis of PA underwent subtype differentiation through computed tomography scanning and adrenal venous sampling (AVS). Of the 12 patients with PA and a subtype diagnosis of an aldosterone producing adenoma, 9 underwent surgical intervention of unilateral adrenalectomy. Samples for EVs isolation and characterization were collected in fasting conditions in heparin-free tubes in the morning just before the AVS, for patients with diagnosis of PA, or at screening for secondary forms of hypertension, for patients with EH; all patients were under treatment with calcium channel blockers or α-blockers, according with ES guideline[1]. Serum was collected after clot formation and immediately processed.

As control groups, we included in the analysis data from 8 healthy normotensive (NT) volunteers and we re-evaluated 4 of the 9 adrenalectomized patients after 1 year of follow-up. For patients with PA, as well as for patients with essential hypertension, we reported sex (male/female), age (years), duration of HTN (years), intensity of anti-hypertensive medication (expressed as defined daily dose; DDD), weight (Kg), BMI (Kg/sqm), systolic and diastolic blood pressure (mmHg), creatinine (mg/dL), GFR (mL/min), glycemia (mg/dL), total cholesterol (mg/dL), triglycerides (mg/dL), HDL (mg/dL), carotid intima-media thickness (cIMT; mm), smoking status (yes/no), diabetes or metabolic syndrome diagnosis (yes/no), theraphy with acetyl-salicylic acid (yes/no) and cardiovascular events (yes/no; we defined as cardiovascular event, the occurrence of sustained arrhythmias [atrial fibrillation, atrial flutter, sustained ventricular tachycardia, and ventricular fibrillation], coronary heart disease [myocardial infarction and unstable angina requiring angioplasty], heart failure requiring hospitalization, stroke [ischemic stroke or transient ischemic attack]; yes/no).

The study was approved by the local ethical committee and fully informed written consent was obtained from each patient.

EV isolation

Blood samples were centrifuged 3,000 g for 30 minutes at room temperature to separate serum from cellular components and then serum was aliquoted and stored at -20°C. EVs were isolated from a 3 mL serum aliquot through a charge-based precipitation method. The serum sample was diluted 1:1 with PBS (Phosphate Buffered Saline) and centrifuged at 3,000 g for 15 minutes at room temperature to remove cell debris, then the supernatant was filtered with 0.2 µm filters and transferred to a sterile tube. A protamine (*Sigma, Saint Louis, Missouri, USA*) / polyethylene glycol (PEG 35,000; *Merck KGaA, Darmstadt, Germany*) solution (250 µL per 1 mL of serum) was added and the mix incubated at 4°C overnight. The following day, samples were centrifuged at 3,000 g for 30 minutes at 22°C to precipitate EVs. The supernatant was removed and samples re-centrifuged at 1,500 g for 5 minutes to remove any remaining supernatant[2]. The pellet was resuspended in 10 mL of PBS and samples were ultra-centrifuged at 100,000 g for 2 hours at 4°C (*Beckman Coulter Optima L-90K; Beckman Coulter, Fullerton, CA, USA*)[3]. The pellet was resuspended in either 100 µL of PBS for transmission electron microscopy (TEM), Nanoparticle Tracking Analysis (NTA)

and Fluorescence-Activated Cell Sorting (FACS) analysis, or 100 µL of RIPA lysis buffer (*Sigma Aldrich, Milan, Italy*) for protein extraction, or 600 µL of Lysis/Binding Buffer (*mirVana Isolation Kit, Thermo Fisher Scientific, Waltham, Massachusetts, USA*) for RNA extraction. Samples were stored at -80°C for RNA extraction and EVs characterization, or -20°C for protein analysis.

EVs characterization

Isolated EVs were visualized by TEM; EVs were loaded on 200 mesh nickel Formvar carbon-coated grids (Electron Microscopy Science, Hatfield, PA, USA) for 20 min, then fixed with 2.5% glutaraldehyde, containing 2% sucrose. Samples were repeatedly washed, negatively stained with NanoVan (Nanoprobes, Yaphank, NY, USA) and then observed using a JEM-1010 electron microscope (Jeol, Tokyo, Japan).

Quantification and size distribution were assessed by NTA using NanoSight LM10 (*NanoSight Ltd, Minton Park, UK*) equipped with a 405 nm laser and Nanoparticle Tracking Analysis NTA 2.3 analytic software[4]; 1 µL for EVs sample was diluted 1:1000 in 999 µL NaCl 0.9% sterile solution and exposed to a laser light source. Brownian movements of EVs were recorded by a camera and size and number of EVs per mL were calculated by Stokes-Einstein equation. Three videos of 30 s were recorded for each sample to perform the analyses.

EVs were further characterized by FACS analysis (*CytoFlex; Beckman Coulter*). A pool of approximately 5×10^{10} particles in 30 µL was incubated for 30 minutes at 4°C with antibodies specific for CD31 (FITC, *Miltenyi; #130-098-171*), CD42b (FITC, *Immuno-Tools; #21330423S*) and CD45 (PE, *CALTAG laboratories; # MHCD4504*). The final volume was increased to 100 µL with PBS and FACS analysis was performed at low flow rate, with 10,000 events using CytoFlex from Beckman Coulter. The instrument was calibrated with Cytoflex Daily QC Fluorospheres according to the manufacturer's instructions followed by Megamix-Plus FSC reagent and FlowCount beads (0.1, 0.3, 0.5, and 0.9 µm; Biocytex; Diagnostica Stago); beads were used to optimize forward and side scatter instrument settings and to gate EVs (gates were set to include particles with a diameter inferior to approximately 1 µM). Buffer alone with antibodies was analyzed prior to sample acquisition to ensure that any background noise was eliminated from the gates used for post-acquisition analysis. Post-acquisition analysis was carried out using CytExpert analysis software (Beckman Coulter).

Finally, a Western Blot for EVs markers was performed on protein lysate. Briefly, EVs were lysed at 4°C for 15 minutes in RIPA lysis buffer supplemented with 1% PMSF, 1% Protease Inhibitor Cocktail, 1% Phosphatase Inhibitor Cocktail 1, and 1% Phosphatase Inhibitor Cocktail 3 (*Sigma Aldrich, St. Louis, MO, USA*). The lysate was sonicated three times for 10 seconds in ice to disrupt EV membranes and extract trans-membrane proteins. Protein concentration was measured by Bradford assay, then samples were loaded on a polyacrylamide 4-15% precast gel (*Mini-PROTEAN® Precast Gels, Bio-Rad, Hercules, California, USA*) at the concentration of 30 µg/well and separated by SDS/PAGE. Proteins were transferred on nitrocellulose membranes by Trans-Blot Turbo Transfer system (*BioRad, Hercules, California, USA*). Membranes were immuno-blotted by polyclonal antibodies anti-CD63 (*Santa Cruz Biotechnologies, Dallas, TX, USA*), TSG101 (Tumor Susceptibility Gene 101; *Santa Cruz Biotechnologies, Dallas, TX, USA*) and Flotillin-1 (*ThermoFisher Scientific, Waltham, Massachusetts, USA*). Protein-bands were detected by chemiluminescent Clarity™ ECL Western Blotting Substrate (*Bio-Rad, Hercules, California, USA*) and analyzed by ChemiDoc System (*Bio-Rad, Hercules, California, USA*). Data were not normalized for any loading endogenous controls because the aim was to demonstrate the presence of EVs markers and not to quantify their expression.

In vitro angiogenic Assay

In vitro formation of capillary-like structures was studied on growth factor-reduced Matrigel (*Corning, Tewksbury, MA, USA*). To evaluate the formation of capillary-like structures, HMEC were washed with PBS, detached with trypsin, and seeded (2×10^4 cells/well) onto Matrigel-coated

wells in EBM, in presence or absence of EVs isolated from PA patients, at the dose of 1.1×10^5 EVs/cell. After 24 hours, cells were observed with a Nikon-inverted microscope (10X) and photographed with a Leica-digital camera. Total length of capillary-like structures was measured by the Angiogenesis Analyzer tool of ImageJ 1.49v software (*NIH*). Bosentan (*Sigma, Saint Louis, Missouri, USA*) was tested at the concentration of 10 μM to counteract the effect of EVs.

Annexin V Apoptosis Assay

HMEC purchased by ATCC (*American Type Culture Collection; Manassas, Virginia, USA*) were plated on 24-well plates at a density of 2×10^4 cells/well in EBM medium (*Lonza, Basilea, Switzerland*) and left to adhere. Cells were incubated with EVs from PA patients, at the dose of 1.1×10^5 EVs/cell. After 24 hours, cells were washed with PBS and harvested with trypsin. Supernatant, PBS used for washing and cells were collected by centrifugation at 400 g for 5 minutes. After removal of the supernatant, cells were resuspended in 100 μL of DMEM. Then 100 μL of Muse Annexin V & Dead Cell Kit reagent (*Merck-Millipore, Darmstadt, Germany*) was added to each sample, cells were mixed and incubated at RT for 20 minutes in the dark. Qualitative and quantitative assessments of apoptosis were conducted with a Muse Cell analyzer (*Merck-Millipore, Darmstadt, Germany*). Ac-YVAD-cmk (*Sigma, Saint Louis, Missouri, USA*) was tested at the concentration of 92.5 μM to counteract the effect of EVs.

Gene expression analysis

mRNA qRT-PCR array profiling was performed on 4 patients diagnosed with PA and 4 with EH, evaluating the expression of a panel of 96 human genes related to endothelial function. The results were subsequently validated with qRT-PCR on 10 patients with PA, 10 with EH (2 patients from each group were included also in qRT-PCR-array analysis), 8 healthy NT controls and 4 post-surgery PA patients.

RNA extraction from purified EVs was performed by mirVana Isolation Kit (*Thermo Fisher Scientific, Waltham, Massachusetts, USA*), according to manufacturer's instructions. RNA concentration was measured by Nanodrop ND-1000 (*Thermo Fisher Scientific, Waltham, Massachusetts, USA*) and the ratio 260/280 and 260/230 showed no contaminations. Genomic DNA was eliminated incubating RNA samples at 42°C for 5 minutes with 2 μL of GE Buffer (*RT² PreAMP cDNA Synthesis kit, Qiagen, Hilden, Germany*) and nuclease-free water to a final volume of 10 μL.

Total RNA (70 ng for each sample included in qRT-PCR-array profiling and 150 ng for qRT-PCR) was retrotranscribed to cDNA with RT² First Strand kit (*Qiagen, Hilden, Germany*) and Veriti Thermal Cycler (*Thermo Fisher Scientific, Waltham, Massachusetts, USA*), according to manufacturer's instructions. cDNA was finally pre-amplified using RT² PreAMP cDNA Synthesis kit (*Qiagen, Hilden, Germany*). Genomic DNA elimination and pre-amplification steps were performed only on samples destined to qRT-PCR-array.

Gene expression profile was evaluated by the Endothelial Cell Biology RT² Profiler PCR Array Format E384 (*Qiagen, Hilden, Germany*), using the real-time thermal cycler QuantStudio 12k flex (*Thermo Fisher Scientific, Waltham, Massachusetts, USA*), according to manufacturer's instructions. Briefly, 102 μL of pre-amplified cDNA for each sample were added to 550 μL of RT² SYBR Green Mastermix and 448 μL of nuclease-free water and then aliquoted into the RT² profiler PCR array. The run method was set as one cycle at 95°C for 10 minutes followed by 40 cycles at 95°C for 15 seconds and 60°C for 60 seconds. Data were analyzed with Applied Biosystems™ interface (*Thermo Fisher ConnectTM, Waltham, Massachusetts, USA*) and Heatmapper software[5], with the $2^{-\Delta\Delta CT}$ relative quantification (RQ) method. Finally, the RQ mean gene expression of PA was compared to EH patients and expressed as fold-change (FC). A gene was considered down-regulated for FC values between 0 and 1 or up-regulated for values greater than 1. Based on results obtained by gene expression profiling and available functional data (see below), the platform was validated through qRT-PCR analysis using specific TaqMan assay for *CASP1* (Caspase 1,

Apoptosis-related Cysteine Peptidase), *EDN1* (Endothelin 1), *F2R* (Coagulation factor II [thrombin] receptor) and *HMOX1* (Heme Oxygenase [decycling] 1) - *RT qPCR Primer Assays: Hs00354836_m1; Hs00174961_m1; Hs00169258_m1; Hs01110250_m1; Thermo Fisher Scientific.* Assays were performed using ABI 7,500 Fast Real-Time PCR System (*Applied Biosystems*), according to manufacturer's instructions. Each sample was run in triplicate. Gene expression levels were analyzed with the $2^{-\Delta\Delta CT}$ relative quantification method, using *18SrRNA* (18S ribosomal RNA) as endogenous control (*RT² qPCR Primer Assays: 4333760T; Thermo Fisher Scientific*).
CASP1 encodes for a cysteine-aspartic acid protease, which is involved in the execution phase of apoptosis and in the initiation of the inflammatory response. Recently, it has been demonstrated that aldosterone is able to induce the up-regulation of *CASP1*, determining vascular dysfunction in mice models[6-8]. In addition, caspase-1 was over-expressed in leucocytes of PA compared to EH patients[8].
END1 encodes for endothelin-1, which is secreted by endothelial cells and acts as vasoconstrictor. ET-1 stimulates aldosterone production in vitro[9], whereas aldosterone induces the release of ET-1 from murine renal collecting duct cells[10]; of note, murine models developed ET-1 mediated vascular remodeling after aldosterone infusion[11].
F2R encodes for the coagulation factor II receptor and play a role in the disruption and maintaining of endothelial barrier integrity[12]; in addition, its genetic variants were associated with the risk of coronary heart disease in a cohort of 1600 hypertensive patients[13].
HMOX1 encodes for heme-oxygenase (decycling) 1, which catabolizes heme but is also associated with an anti-inflammatory response; mechanistically, HMOX1 catabolizes free heme, producing CO, which induces the expression of the anti-inflammatory IL-10 and IL-1 receptor antagonists[14]; consistently, *HMOX1* was up-regulated, probably to counteract fibrosis, oxidative stress and DNA damage in livers of aldosterone-treated murine models[15]. Finally, the expression of *HMOX1* was also higher in APA compared to the adjacent normal adrenal tissue[16].
We also performed a qRT-PCR for *CASP1*, *EDN1*, *F2R* and *HMOX1* on RNA extracted from human microvascular endothelial cells (HMECs) after 24 hours EVs-treatment. The RQ mean gene expression of HMEC treated with serum-derived EVs was compared with non-treated cells (used as negative control, Ctrl, and set to 1).

Statistical Analysis
IBM SPSS Statistics 22 (*IBM Corp., Armonk, New York, USA*) and GraphPad PRISM 7.0a (*La Jolla, California, USA*) were used for statistical analyses. Data for scalar variables were analyzed with the Kolmogorov–Smirnov test to determine their distributions. Normally distributed variables are expressed as mean ± standard deviation; non-normally distributed variables are expressed as median [interquartile range]. ANOVA one-way and Mann-Whitney's tests were used to compare variables with a normal or non-normal distribution, respectively. Categorical variables are expressed as absolute number (percentage) and were compared through a chi square test (Fisher's exact test when sample size was ≤ 5). Correlations were evaluated by Pearson test (R coefficient) and regression curve analysis. *P*-values of less than 0.05 were considered significant.

REFERENCES

44. Funder JW, Carey RM, Mantero F, Murad MH, Reincke M, Shibata H, Stowasser M, Young WF Jr. The Management of Primary Aldosteronism: Case Detection, Diagnosis, and Treatment: An Endocrine Society Clinical Practice Guideline. *J Clin Endocrinol Metab*. 2016;101:1889-1916.
45. Deregibus MC, Figliolini F, D'Antico S, Manzini PM, Pasquino C, De Lena M, Tetta C, Brizzi MF, Camussi G. Charge-based precipitation of extracellular vesicles. *Int J Mol Med*. 2016;38:1359-1366.
46. Witwer KW, Buzás EI, Bemis LT, Bora A, Lässer C, Lötvall J, Nolte-'t Hoen EN, Piper MG, Sivaraman S, Skog J, Théry C, Wauben MH, Hochberg F. Standardization of sample collection, isolation and analysis methods in extracellular vesicle research. *J Extracell Vesicles*. 2013 27;2.
47. Dragovic RA, Gardiner C, Brooks AS, Tannetta DS, Ferguson DJ, Hole P, Carr B, Redman CW, Harris AL, Dobson PJ, Harrison P, Sargent IL. Sizing and phenotyping of cellular vesicles using Nanoparticle Tracking Analysis. *Nanomedicine*. 2011;7:780-788.
48. Babicki S, Arndt D, Marcu A, Liang Y, Grant JR, Maciejewski A, Wishart DS. Heatmapper: web-enabled heat mapping for all. *Nucleic Acids Res*. 2016;44:147-153.
49. Kadoya H, Satoh M, Sasaki T, Taniguchi S, Takahashi M, Kashihara N. Excess aldosterone is a critical danger signal for inflammasome activation in the development of renal fibrosis in mice. *FASEB J*. 2015;29:3899-3910.
50. Ding W, Guo H, Xu C, Wang B, Zhang M, Ding F. Mitochondrial reactive oxygen species-mediated NLRP3 inflammasome activation contributes to aldosterone-induced renal tubular cells injury. *Oncotarget*. 2016;7:17479-17491.
51. Bruder-Nascimento T, Ferreira NS, Zanotto CZ, et al. NLRP3 Inflammasome Mediates Aldosterone-Induced Vascular Damage. *Circulation*. 2016;134:1866-1880.
52. Rossi GP, Andreis PG, Neri G, Tortorella C, Pelizzo MR, Sacchetto A, Nussdorfer GG. Endothelin-1 stimulates aldosterone synthesis in Conn's adenomas via both A and B receptors coupled with the protein kinase C- and cyclooxygenase-dependent signaling pathways. *J Investig Med*. 2000;48:343-350.
53. Welch AK, Jeanette Lynch I, Gumz ML, Cain BD, Wingo CS. Aldosterone alters the chromatin structure of the murine endothelin-1 gene. *Life Sci*. 2016;159:121-126.
54. Pu Q, Neves MF, Virdis A, Touyz RM, Schiffrin EL. Endothelin antagonism on aldosterone-induced oxidative stress and vascular remodeling. *Hypertension*. 2003;42:49-55.
55. Feistritzer C, Riewald M. Endothelial barrier protection by activated protein C through PAR1-dependent sphingosine 1-phosphate receptor-1 crossactivation. Blood. 2005;105:3178-3184.
56. Gigante B, Bellis A, Visconti R, Marino M, Morisco C, Trimarco V, Galasso G, Piscione F, De Luca N, Prince JA, de Faire U, Trimarco B. Retrospective analysis of coagulation factor II receptor (F2R) sequence variation and coronary heart disease in hypertensive patients. Arterioscler Thromb Vasc Biol. 2007;27:1213-1219.
57. Piantadosi CA, Withers CM, Bartz RR, MacGarvey NC, Fu P, Sweeney TE, Welty-Wolf KE, Suliman HB. Heme oxygenase-1 couples activation of mitochondrial biogenåesis to anti-inflammatory cytokine expression. J Biol Chem. 2011 May 6;286(18):16374-85.
58. Queisser N, Happ K, Link S, Jahn D, Zimnol A, Geier A, Schupp N. Aldosterone induces fibrosis, oxidative stress and DNA damage in livers of male rats independent of blood pressure changes. Toxicol Appl Pharmacol. 2014 Nov 1;280(3):399-407.
59. Calò LA, Pagnin E, Davis PA, Armanini D, Mormino P, Rossi GP, Pessina AC. Oxidative stress-related proteins in a Conn's adenoma tissue. Relevance for aldosterone's prooxidative and proinflammatory activity. J Endocrinol Invest. 2010 Jan;33(1):48-53.

SUPPLEMENTAL TABLE S1

	Variable	Male	Female	*P*-Value
ALL (n=32)	n° EVs/mL	6.3E+11 (1.3E+11-2.1E+12)	2.7E+11 (1.3E+11-6.6E+11)	0.190
	Diameter (nm)	231 (191-259)	246 (196-287)	0.287
	TOT n° Events/60sec	6765 (4924-9053)	3728 (3131-6833)	0.051
	CD31 n° Events/60sec	1093 (599-1809)	996 (590-1252)	0.621
	CD42b n° Events/60sec	747 (564-1116)	524 (382-853)	0.109
	CD45 n° Events/60sec	2042 (1229-4293)	1482 (1126-2390)	0.408
	CASP1 (Rq)	1.2 (0.1-8.4)	1.1 (0.1-5.4)	0.308
	EDN1 (Rq)	1.0 (0.1-10.6)	1.8 (0.2-13.3)	0.382
	F2R (Rq)	1.6 (0.4-6.4)	7.5 (0.3-30.0)	0.524
	HMOX1 (Rq)	1.8 (1.0-10.0)	4.0 (0.8-7.6)	0.724
NT (n=8)	n° EVs/mL	1.2E+11 (4.3E+10-2.3E+11)	1.2E+11 (1,1E+11-1.2E+11)	0.857
	Diameter (nm)	230 (210-269)	295 (295-296)	0.071
	TOT n° Events/60sec	6608 (5100-7745)	3728 (3008-3728)	0.071
	CD31 n° Events/60sec	925 (565-1081)	863 (773-863)	0.857
	CD42b n° Events/60sec	676 (403-876)	551 (328-551)	0.643
	CD45 n° Events/60sec	1632 (1414-1984)	1113 (769-1113)	0.429
	CASP1 (Rq)	0.6 (0.1-1.7)	0.1 (0.01-0.1)	0.071
	EDN1 (Rq)	0.5 (0.1-3.3)	6.7 (0.2-6.7)	0.429
	F2R (Rq)	2.8 (1.2-6.4)	4.0 (0.1-4.0)	1.000
	HMOX1 (Rq)	1.2 (0.5-3.0)	0.5 (0.1-0.5)	0.286
EH (n=12)	n° EVs/mL	7.4E+11 (2.0E+11-2.6E+12)	1.9E+11 (1.4E+11-3.1E+11)	0.154
	Diameter (nm)	225 (186-261)	246 (209-275)	0.368
	TOT n° Events/60sec	5400 (2449-6945)	3127 (2355-3833)	0.257
	CD31 n° Events/60sec	882 (499-1537)	645 (489-924)	0.762
	CD42b n° Events/60sec	836 (525-1613)	366 (254-609)	0.107
	CD45 n° Events/60sec	2071 (924-3862)	1460 (1066-1759)	0.610
	CASP1 (Rq)	0.7 (0.1-6.6)	2.3 (0.1-4.9)	0.762
	EDN1 (Rq)	0.2 (0.1-1.2)	1.6 (0.4-25.3)	0.171
	F2R (Rq)	1.3 (0.3-8.0)	0.4 (0.1-32.2)	0.762
	HMOX1 (Rq)	1.8 (0.9-6.6)	5.9 (3.5-15.2)	0.114
PA (n=12)	n° EVs/mL	1.5E+12 (7.4E+11-6.6E+12)	6.8E+11 (5.9E+11-8.3E+11)	0.073
	Diameter (nm)	251 (173-259)	215 (172-261)	0.933
	TOT n° Events/60sec	9548 (6116-11922)	7643 (5801-8933)	0.610
	CD31 n° Events/60sec	1787 (779-2514)	1545 (1161-1958)	0.762
	CD42b n° Events/60sec	764 (554-1432)	808 (631-924)	1.000
	CD45 n° Events/60sec	3359 (1125-5265)	3091 (1970-4351)	1.000
	CASP1 (Rq)	11.3 (6.0-20.0)	4.1 (0.8-10.6)	0.257
	EDN1 (Rq)	14.5 (1.7-40.3)	4.9 (0.4-12.3)	0.257
	F2R (Rq)	1.9 (0.4-22.2)	17.7 (7.7-46.0)	0.171
	HMOX1 (Rq)	10.3 (7.3-17.4)	4.0 (0.6-8.8)	0.067

Supplemental Table S1 – Serum-derived EVs characterization, stratified for sex (male *versus* female) and diagnosis (normotensive controls *versus* EH patients *versus* PA patients). The table report NTA, FACS and qRT-PCR data. NT, Normotensive healthy controls; EH, Essential Hypertension; PA, Primary Aldosteronism.

SUPPLEMENTAL TABLE S2

Gene	UniGene	GenBank	Description	Angiogenesis	Vasoreactivity	Inflammation	Apoptosis	Cell Adhesion	Coagulation	Platelet Activation
ACTB	Hs.520640	NM_001101	Actin, beta							
B2M	Hs.534255	NM_004048	Beta-2-microglobulin							
GAPDH	Hs.592355	NM_002046	Glyceraldehyde-3-phosphate dehydrogenase							
HPRT1	Hs.412707	NM_000194	Hypoxanthine phosphoribosyltransferase 1							
RPLP0	Hs.546285	NM_001002	Ribosomal protein, large, P0							
ACE	Hs.654434	NM_000789	Angiotensin I converting enzyme 1		✔	✔				
AGT	Hs.19383	NM_000029	Angiotensinogen		✔	✔		✔		
ALOX5	Hs.89499	NM_000698	Arachidonate 5-lipoxygenase		✔	✔				
ANGPT1	Hs.369675	NM_001146	Angiopoietin 1	✔						
ANXA5	Hs.480653	NM_001154	Annexin A5				✔		✔	
APOE	Hs.654439	NM_000041	Apolipoprotein E		✔	✔				✔
BAX	Hs.624291	NM_004324	BCL2-associated X protein				✔			
BCL2	Hs.150749	NM_000633	B-cell CLL/lymphoma 2				✔	✔		
BCL2L1	Hs.516966	NM_138578	BCL2-like 1				✔			
CALCA	Hs.37058	NM_001741	Calcitonin-related polypeptide alpha		✔	✔		✔		
CASP1	Hs.2490	NM_033292	Caspase 1, apoptosis-related cysteine peptidase				✔			
CCL2	Hs.303649	NM_002982	Chemokine (C-C motif) ligand 2	✔		✔	✔			
CCL5	Hs.514821	NM_002985	Chemokine (C-C motif) ligand 5	✔		✔	✔			
CDH5	Hs.76206	NM_001795	Cadherin 5, type 2 (vascular endothelium)					✔		
CFLAR	Hs.390736	NM_003879	CASP8 and FADD-like apoptosis regulator				✔			
COL18A1	Hs.517356	NM_030582	Collagen, type XVIII, alpha 1					✔		
CX3CL1	Hs.531668	NM_002996	Chemokine (C-X3-C motif) ligand 1	✔	✔	✔	✔	✔		✔
EDN1	Hs.511899	NM_001955	Endothelin 1	✔	✔		✔		✔	
EDN2	Hs.1407	NM_001956	Endothelin 2		✔					
EDNRA	Hs.183713	NM_001957	Endothelin receptor type A	✔	✔	✔	✔			
ENG	Hs.76753	NM_000118	Endoglin	✔				✔		
F2R	Hs.482562	NM_001992	Coagulation factor II (thrombin) receptor		✔	✔			✔	✔
F3	Hs.62192	NM_001993	Coagulation factor III (thromboplastin)	✔		✔			✔	
FGF2	Hs.284244	NM_002006	Fibroblast growth factor 2 (basic)	✔			✔			
FN1	Hs.203717	NM_002026	Fibronectin 1	✔		✔		✔	✔	✔
HIF1A	Hs.597216	NM_001530	Hypoxia inducible factor 1, alpha subunit	✔		✔	✔			
HMOX1	Hs.517581	NM_002133	Heme oxygenase (decycling) 1	✔	✔	✔	✔			
ICAM1	Hs.643447	NM_000201	Intercellular adhesion molecule 1		✔			✔		
IL11	Hs.467304	NM_000641	Interleukin 11							✔
IL3	Hs.694	NM_000588	Interleukin 3				✔			
IL6	Hs.654458	NM_000600	Interleukin 6	✔		✔	✔			✔
IL7	Hs.591873	NM_000880	Interleukin 7				✔			
ITGA5	Hs.505654	NM_002205	Integrin, alpha 5	✔				✔		
ITGAV	Hs.436873	NM_002210	Integrin, alpha V	✔				✔		
ITGB1	Hs.643813	NM_002211	Integrin, beta 1	✔				✔		
ITGB3	Hs.218040	NM_000212	Integrin, beta 3	✔				✔		✔
KIT	Hs.479754	NM_000222	V-kit Hardy-Zuckerman 4	✔						
KLK3	Hs.171995	NM_001648	Kallikrein-related peptidase 3	✔						
MMP1	Hs.83169	NM_002421	Matrix metallopeptidase 1						✔	
MMP2	Hs.513617	NM_004530	Matrix metallopeptidase 2	✔						
MMP9	Hs.297413	NM_004994	Matrix metallopeptidase 9	✔						
NOS3	Hs.707978	NM_000603	Nitric oxide synthase 3	✔	✔					✔
NPPB	Hs.219140	NM_002521	Natriuretic peptide B	✔	✔	✔				
PDGFRA	Hs.74615	NM_006206	PLT-derived GF receptor, alpha polypeptide					✔		✔

PF4	Hs.81564	NM_002619	Platelet factor 4	✓			✓		✓	✓
PGF	Hs.252820	NM_002632	Placental growth factor	✓						
PLAU	Hs.77274	NM_002658	Plasminogen activator, urokinase	✓				✓	✓	
PLG	Hs.143436	NM_000301	Plasminogen					✓	✓	✓
PTGIS	Hs.302085	NM_000961	Prostaglandin I2 synthase		✓					
PTGS2	Hs.196384	NM_000963	Prostaglandin-endoperoxide synthase 2	✓	✓					
SELE	Hs.89546	NM_000450	Selectin E			✓		✓		
SERPINE1	Hs.414795	NM_000602	Serpin peptidase inhibitor, clade E member 1	✓				✓	✓	✓
SOD1	Hs.443914	NM_000454	Superoxide dismutase 1, soluble		✓					✓
SPHK1	Hs.68061	NM_021972	Sphingosine kinase 1	✓		✓	✓			
TEK	Hs.89640	NM_000459	TEK tyrosine kinase, endothelial	✓			✓		✓	
TFPI	Hs.516578	NM_006287	Tissue factor pathway inhibitor						✓	
THBD	Hs.2030	NM_000361	Thrombomodulin						✓	✓
THBS1	Hs.164226	NM_003246	Thrombospondin 1	✓		✓	✓	✓	✓	✓
TNF	Hs.241570	NM_000594	Tumor necrosis factor			✓	✓	✓		
TNFSF10	Hs.478275	NM_003810	Tumor necrosis factor superfamily, member 10				✓			
VCAM1	Hs.109225	NM_001078	Vascular cell adhesion molecule 1			✓		✓		
VEGFA	Hs.73793	NM_003376	Vascular endothelial growth factor A	✓				✓		✓
VWF	Hs.440848	NM_000552	Von Willebrand factor					✓	✓	✓

Supplemental Table S2 – Genes expressed in EVs of at least 1 patient (independently from diagnosis) on mRNA qRT-PCR-array profiling platform. The table reports description and function for each gene.

SUPPLEMENTAL FIGURE S1

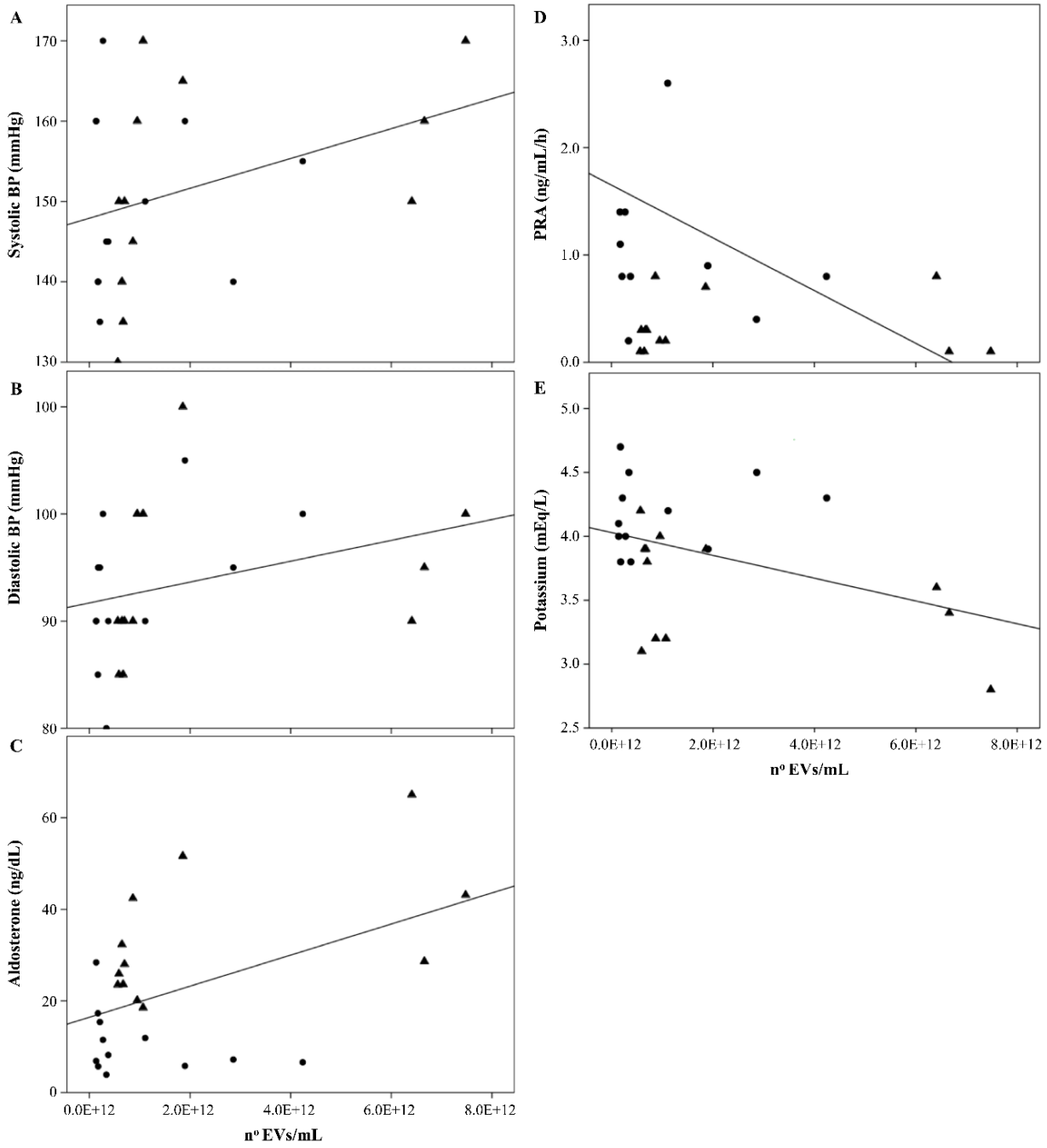

Supplemental Figure S1 – Regression lines and correlation coefficients between number of EVs per mL at the NTA and Systolic BP, Diastolic BP, Aldosterone, PRA and potassium; the analysis was performed on patients diagnosed with primary aldosteronism (PA; n = 12) or essential hypertension (EH; n = 12). (A) Systolic BP (mmHg) *versus* EV n° per mL regression line: R = 0.347; *P*-value = 0.097; Y = $1.48E^{+2} + 1.86E^{-12}$ * X; (B) Diastolic BP (mmHg) *versus* n° EVs/mL regression line: R = 0.398; *P*-value = 0.144; Y = $0.92E^{+2} + 9.73E^{-13}$ * X; (C) Aldosterone (ng/dL) *versus* n° EVs/mL regression line: R = 0.472; *P*-value = 0.020; Y = $0.16E^{+2} + 3.39E^{-11}$ * X; (D) PRA (ng/mL/h) *versus* n° EVs/mL regression line: R = -0.255; *P*-value = 0.229; Y = 1.65 - $2.46E^{-13}$ * X; (E) Potassium (mEq/L) *versus* n° EVs/mL regression curve: R = -0.419; *P*-value = 0.041; Y = 4.03 – $8.92E^{-14}$ * X. Circles: EH patients; Triangles: PA patients. BP, Blood Pressure; PRA, Plasma Renin Activity.

SUPPLEMENTAL FIGURE S2

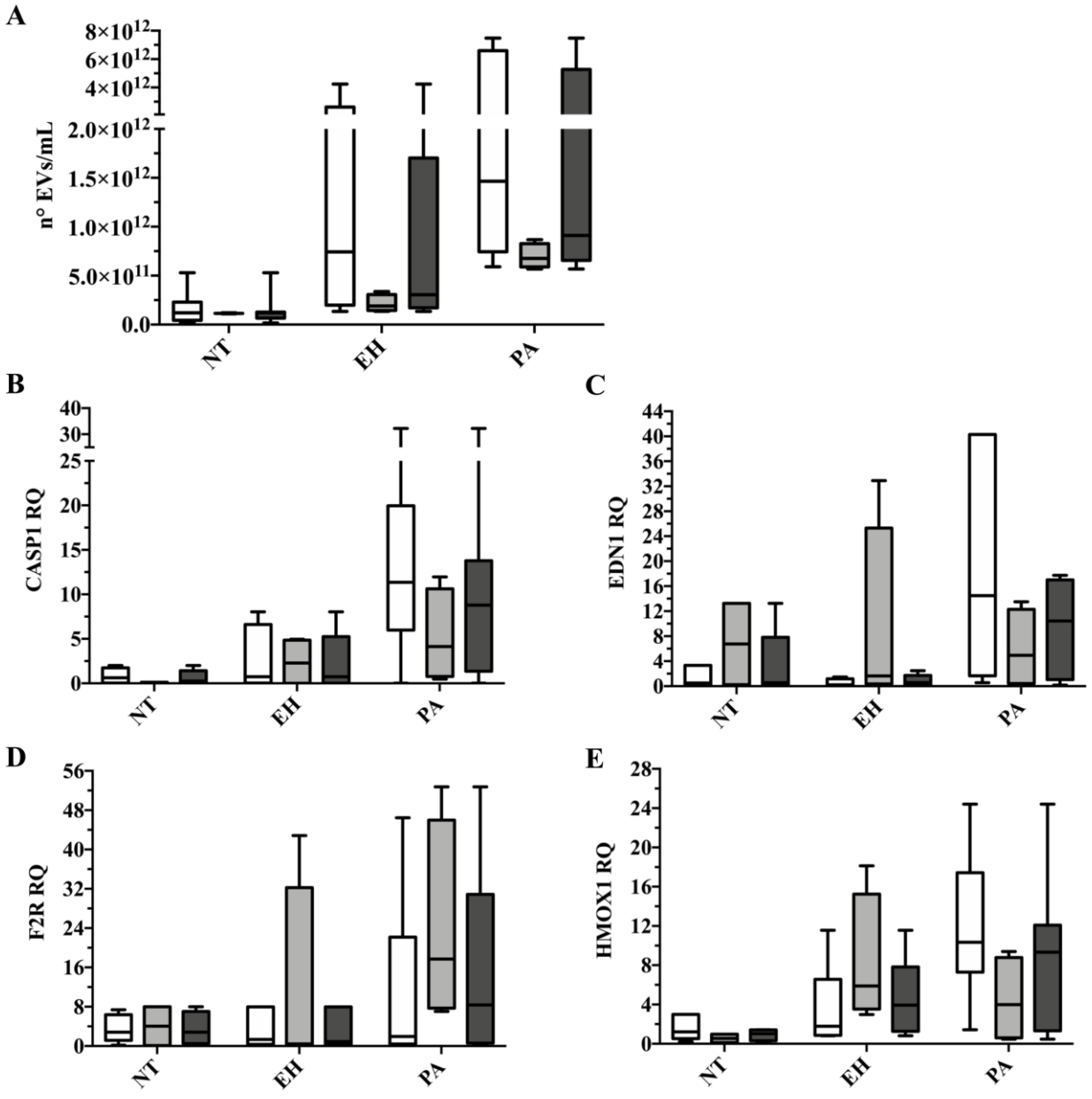

Supplemental Figure S2 – Serum-derived EVs characterization (NTA and qRT-PCR analysis), stratified for sex: male (white boxes) *versus* female (light grey boxes); dark grey boxes represent the entire cohort. (A) Quantification of EVs (n° EVs per mL) at NTA in male *versus* female patients stratified for diagnosis (NT, Normotensive controls; EH, Essential Hypertension; PA, Primary Aldosteronism); (B, C, D, E) Gene expression profile by qRT-PCR stratified for sex and diagnosis (NT *versus* EH *versus* PA). *CASP1*, *EDN1*, *F2R* and *HMOX1* levels were evaluated using *18SrRNA*, as endogenous reference gene. RQ (Relative Quantification) are corrected for the n° of EVs/mL for each sample. The horizontal line indicates the median and box and bar represent the 25th to 75th and the 5th to 95th percentiles, respectively.